Dynamic Optical Lattices of Subwavelength Spacing for Ultracold Atoms

Sylvain Nascimbene,[1,*] Nathan Goldman,[1,2] Nigel R. Cooper,[3] and Jean Dalibard[1]
[1]Laboratoire Kastler Brossel, Collège de France, ENS-PSL Research University, CNRS, UPMC-Sorbonne Universités, 11 place Marcelin Berthelot, 75005 Paris, France
[2]CENOLI, Faculté des Sciences, Université Libre de Bruxelles (ULB), B-1050 Brussels, Belgium
[3]T.C.M. Group, Cavendish Laboratory, J.J. Thomson Avenue, Cambridge CB3 0HE, United Kingdom
(Received 1 June 2015; published 2 October 2015)

We propose a scheme for realizing lattice potentials of subwavelength spacing for ultracold atoms. It is based on spin-dependent optical lattices with a time-periodic modulation. We show that the atomic motion is well described by the combined action of an effective, time-independent lattice of small spacing, together with a micromotion associated with the time modulation. A numerical simulation shows that an atomic gas can be adiabatically loaded into the effective lattice ground state, for time scales comparable to the ones required for adiabatic loading of standard optical lattices. We generalize our scheme to a two-dimensional geometry, leading to Bloch bands with nonzero Chern numbers. The realization of lattices of subwavelength spacing allows for the enhancement of energy scales, which could facilitate the achievement of strongly correlated (topological) states.

DOI: 10.1103/PhysRevLett.115.140401 PACS numbers: 03.75.Hh, 37.10.Jk, 67.85.-d

Optical lattices have allowed experiments on ultracold atomic gases to investigate a large range of lattice models of quantum many-body physics [1]. Their development led to the realization of strongly correlated states of matter, such as bosonic and fermionic Mott insulators, and low-dimensional gases [2]. In its simplest form, an optical lattice consists of the optical dipole potential associated with a standing wave of retroreflected laser light. It can be described as a periodic potential $V(x) = U_0 \cos^2(kx)$, of spatial period $d = \lambda/2$, where λ is the laser wavelength and $k = 2\pi/\lambda$. More complex optical lattices, such as superlattices [3,4] or two-dimensional honeycomb lattices [5,6], can be generated with suitable laser configurations. The recoil energy $E_r = h^2/(8md^2)$, where h is Planck's constant and m is the atom mass, sets the natural energy scale for elementary processes, such as atom tunneling between neighboring lattice sites, as well as the temperature range $T \lesssim E_r/k_B \sim 100$ nK, typically required for quantum degeneracy.

For a large class of models, the physical behavior is dictated by processes associated with even much smaller energies, such as superexchange or magnetic dipole interactions [1]. The associated temperature scales remain out of reach in current experiments. In order to circumvent this limitation, it is desirable to find novel schemes for generating optical lattices with spacing $d_{\mathrm{eff}} \ll \lambda$, in order to enhance the associated energy scale $E_r^{\mathrm{eff}} = h^2/(8md_{\mathrm{eff}}^2)$ [7]. Schemes have been proposed to generate lattices of subwavelength spacing, based on multiphoton optical transitions [8] or on adiabatic dressing of state-dependent optical lattices [7]; the realization of lattices with spacing $d_{\mathrm{eff}} = \lambda/4$ was reported in Ref. [9]. An interesting alternative would be to trap atomic gases in the electromagnetic fields of nanostructured condensed-matter systems [10–12].

In this Letter, we propose a novel scheme leading to lattices of spacing $d_{\mathrm{eff}} = d/N$, with N being an arbitrary integer, based on spin-dependent lattices with time-periodic modulation. In the regime of large modulation frequency [13–16], the atom dynamics is governed by an effective static periodic potential of spacing d_{eff}, with an additional micromotion. This description is confirmed by a numerical simulation, which shows the possibility of loading adiabatically the ground state of the effective lattice and to perform Bloch oscillations. We discuss the extension of the scheme to two-dimensional lattices with nontrivial topology. Lattices with artificial magnetic fields, generally leading to topological bands, were recently realized in experiments, with standard lattice spacing [17]. For those systems, increasing the energy scale using short-spacing lattices could prove important for creating strongly correlated states such as fractional Chern insulators [18,19].

A basic scheme of our method is pictured in Fig. 1. Consider a periodic potential $V(x)$ of period d, which is abruptly shifted by the distance d/N at stroboscopic times $t_n = (n/N)T$, $n \in \mathbb{Z}$, leading to a time-periodic potential $V(x,t)$ of period T. Provided that T is much smaller than typical time scales of atomic motion, the atoms experience an effective time-averaged potential $V_{\mathrm{eff}}(x) = \int V(x,t)dt/T$. A simple calculation shows that $V_{\mathrm{eff}}(x)$ is given by the sum of all harmonics of the potential $V(x)$, whose orders are multiples of N [20]. The effective potential $V_{\mathrm{eff}}(x)$ is thus spatially periodic, of spatial period $d_{\mathrm{eff}} = d/N$.

Conventional optical lattices present a spatial modulation proportional to the intensity pattern of interfering light

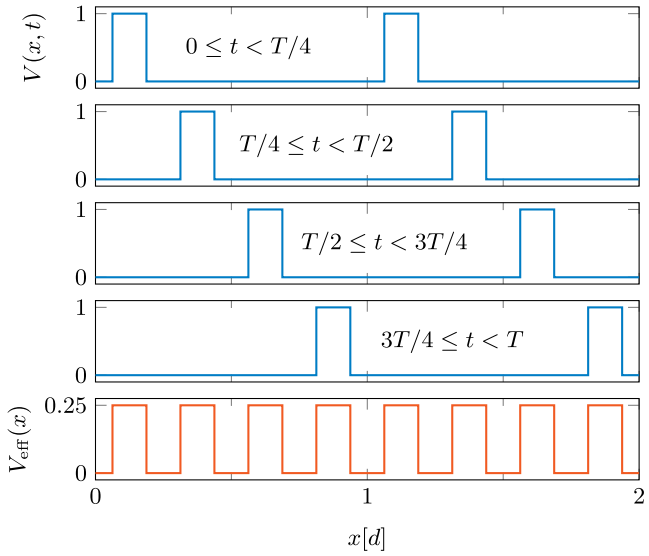

FIG. 1 (color online). Stroboscopic scheme for engineering short-spacing lattices, illustrated in the case $N = 4$. We make use of a periodic potential $V(x,t)$ of spatial period d that is shifted by the distance d/N after every time step of duration T/N (the blue curves). The effective potential $V_{\text{eff}}(x)$ (the red curve), resulting from time averaging, exhibits a spatial period $d_{\text{eff}} = d/N$.

waves, which exhibit spatial frequencies of at most twice the light momentum k. Thus, applying the stroboscopic scheme in Fig. 1 to these potentials could not lead to effective lattices of period $d_{\text{eff}} < \lambda/2$. This restriction does not apply to spinful particles subjected to spin-dependent optical lattices. As an illustration, consider a spin-1/2 particle evolving in the potential $V(x) = V_L \cos(2kx)\sigma_z + V_B\sigma_x$, where σ_u ($u = x, y, z$) are the Pauli matrices. In a dressed state picture, the atom may follow adiabatically the state of lowest energy $V_-(x) = -\sqrt{V_L^2\cos^2(2kx) + V_B^2}$. As this potential exhibits harmonics of the spatial frequency $2k$ of all orders, the lattice spacings achievable by applying the stroboscopic scheme to $V_-(x)$ can be made arbitrarily small.

We describe in the following a modified, more practical version of this scheme, which consists of a spin-dependent optical lattice with smooth temporal variations, given by

$$V(x,t) = V_L \cos(2kx - \Omega t)\sigma_z + V_B \cos(N\Omega t)\sigma_x. \quad (1)$$

This potential satisfies $V(x + d/N, t + T/N) = V(x,t)$, with $d = \pi/k$; thus, it can be viewed as a continuous version of the stroboscopic scheme. Understanding the physical effects of the potential (1) falls within the description of time-periodic Hamiltonian systems [13–16]. Following Ref. [15], we describe the dynamics of an atom between the times t_i and t_f as

$$U(t_i \to t_f) = e^{-iK(t_f)} e^{-(i/\hbar)(t_f - t_i)H_{\text{eff}}} e^{iK(t_i)}, \quad (2)$$

where we introduce a time-independent effective Hamiltonian H_{eff} and a time-periodic kick operator $K(t)$. The three operators in Eq. (2) describe, from right to left, the role of the initial phase of the Hamiltonian at time t_i, the evolution from t_i to t_f according to a stationary Hamiltonian, and the micromotion related to the final phase of the Hamiltonian at time t_f.

The expressions for the effective Hamiltonian H_{eff} and the kick operator $K(t)$ can be calculated through a perturbative expansion in powers of $1/\Omega$; see Refs. [14,15]. To lowest order, this yields

$$H_{\text{eff}} = \frac{p^2}{2m} + V_{\text{eff}}(x), \quad (3)$$

$$V_{\text{eff}}(x) = \frac{U_{\text{eff}}}{2}\cos(2Nkx)\sigma_x,$$

$$U_{\text{eff}} = \frac{2V_B}{N!}\left(\frac{V_L}{\hbar\Omega}\right)^N, \quad (4)$$

$$K(t) = \frac{-V_L}{\hbar\Omega}\sin(2kx - \Omega t)\sigma_z + \frac{V_B}{N\hbar\Omega}\sin(N\Omega t)\sigma_x. \quad (5)$$

The effective potential (4), which describes a periodic potential of depth U_{eff} and spatial period $d_{\text{eff}} = d/N$, was derived under the assumption that N is an even integer (a similar potential is found for N odd). The expression (4) has been obtained based on a Born-Oppenheimer approximation, in which the kinetic energy term is neglected and one calculates the effective potential for a given position x, treating internal degrees of freedom (σ_j operators) quantum mechanically. One finds that the terms neglected here are smaller than those given in Eq. (4), by a factor $E_r/(\hbar\Omega) \ll 1$. Furthermore, this approximation is validated by a direct comparison with the full quantum treatment (see below). In the Supplemental Material [20] we show that the perturbative expansion can be resumed, with respect to either the variable $V_L/(\hbar\Omega)$ or $V_B/(\hbar\Omega)$. There, we also discuss the generalization of this modulation scheme to an arbitrary spin F, through the substitution $\sigma_u \to 2F_u$ [20].

In order to test the validity of the effective Hamiltonian (3), we performed a numerical study of the full time-periodic Hamiltonian using the Floquet formalism. Since the Hamiltonian H is invariant under the symmetries $\mathcal{T}_x$: $x \to x + d$ and $\mathcal{T}_t$: $t \to t + T$, we look for eigenstates written as Bloch-Floquet wave functions $\psi_{q,\omega}(x,t) = e^{i(qx-\omega t)}u_{q,\omega}(x,t)$, where $u_{q,\omega}(x,t)$ is d periodic in x and T periodic in t [24,25]. Eigenstates are labeled by their quasimomentum $-k < q \le k$ and quasienergy $0 \le \hbar\omega < \hbar\Omega$. An example of the band structure calculated numerically for $N = 4$ is plotted in Fig. 2(a). The band structure exhibits gap openings once every four bands, at the momenta Nkp, where $p \in \mathbb{Z}^*$, as expected for a lattice of spacing d/N.

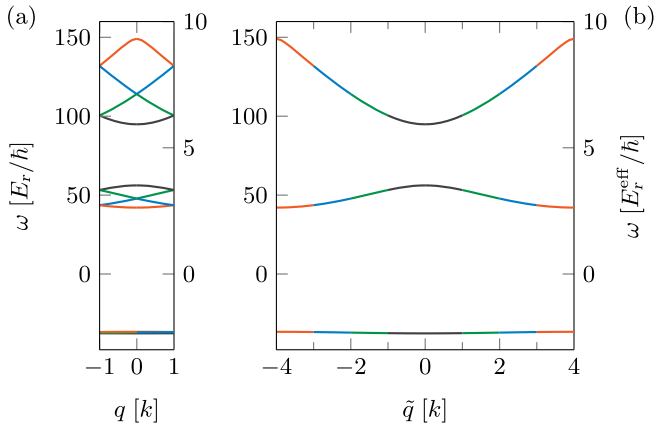

FIG. 2 (color online). Band structure of a dynamic optical lattice of spacing $d_{\rm eff} = d/4$, corresponding to the parameters $N = 4$, and $V_L = V_B = \hbar\Omega = 200E_r^{\rm eff}$. In (a), we make use of the spatial and temporal translational symmetries $\mathcal{T}_x$, $\mathcal{T}_t$ and label the eigenstates by their quasimomentum $-k \le q < k$ and quasienergy $-\hbar\Omega/2 \le \hbar\omega < \hbar\Omega/2$. The Bloch-Floquet bands can be unfolded using the additional symmetry $\mathcal{T}^*$, leading to the band structure in (b), indexed by the modified quasimomentum $-4k \le \tilde{q} < 4k$. The unfolding of the band structure can be followed from the different coloring of successive bands.

The band structure can be unfolded, making use of the additional symmetry $\mathcal{T}^*$: $x \to x + d/N, t \to t + T/N$. As explained in the Supplemental Material [20], eigenstates associated with the symmetries $\mathcal{T}_x$, $\mathcal{T}_t$, and $\mathcal{T}^*$ can be written as $\psi_{\tilde{q},\omega}(x,t) = e^{i(\tilde{q}x-\omega t)}v_{\tilde{q},\omega}(x,t)$, where $v_{\tilde{q},\omega}(x,t)$ is d/N periodic in x and 2π periodic in $(kx - \Omega t)$. We show the band structure calculated within this formalism in Fig. 2(b), which is very close to that expected for a lattice of spacing d/N and depth $U_{\rm eff} \simeq 10.9E_r^{\rm eff}$ [26].

The practical relevance of the short-spacing lattice described above is based on the ability to load atoms into the ground state of the effective potential (4). The analysis of this loading protocol requires special care, as the effective-Hamiltonian approach inherent to Eq. (2) assumes a constant lattice depth [15]. In fact, we find that the concept of the effective Hamiltonian can be modified so as to describe the time evolution under a ramp of the moving-lattice depth V_L; see Ref. [20]. We simulate the lattice loading from a numerical calculation of the full dynamics of an atomic wave packet under the action of the potential (1). Starting from a Gaussian wave packet, spin polarized along x, we solve the Schrödinger equation, discretized in space and time, with a lattice depth V_L slowly ramped up for a duration $t_{\rm ramp}$. As shown in Fig. 3(a), a ramp duration $t_{\rm ramp} = 20\hbar/E_r^{\rm eff}$ leads to a state with strong spatial modulations of spacing d/N, as expected for a wave packet prepared in the lowest band of the effective lattice (4). The calculated population in the effective lowest band is 93%, close to the value expected with standard optical lattices for such a ramp duration. In the Supplemental Material [20] we analyze the momentum distribution, which corresponds to the one expected for the ground state of the effective lattice, slightly modified by the micromotion.

The system description as an effective d/N lattice is also supported by a numerical simulation of Bloch oscillations. We calculate the action of a linear potential $-Fx$ applied to the state obtained after the lattice loading. As shown in Figs. 3(b) and 3(c), the wave packet undergoes Bloch oscillations, revealed as real-space oscillations of its center of mass. Both the amplitude and the period of this oscillation agree well with those expected for an effective lattice of period d/N and depth $U_{\rm eff}$ inferred from band structure calculations.

The potential $V(x,t)$ written in Eq. (1) corresponds to the sum of a time-modulated magnetic field and a spin-dependent optical lattice moving at the velocity $v_{\rm latt} = \Omega/(2k)$. In the above discussion we considered the effect of this potential as an effective static optical lattice. An alternative view is obtained in the frame of

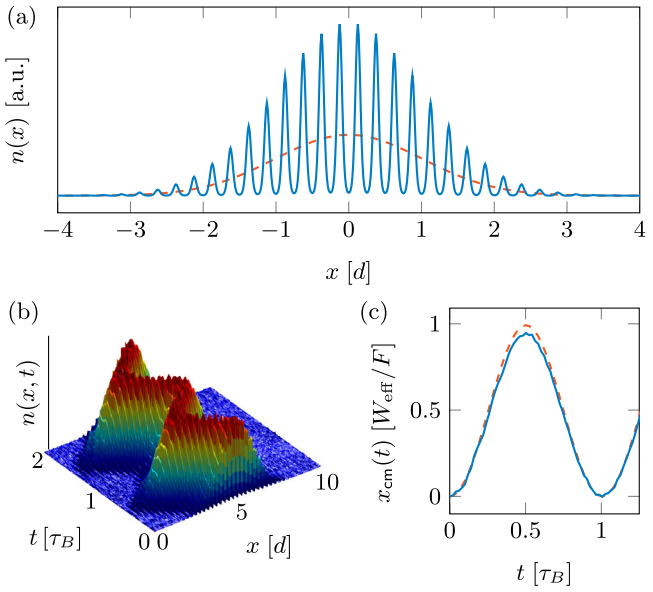

FIG. 3 (color online). (a) Atomic density of a wave packet loaded into a dynamic lattice of spacing $d_{\rm eff} = d/4$. We start from a Gaussian wave packet, spin polarized along x, of wave function $\psi(x, t = 0) = \exp[-x^2/(2\sigma^2)]$, with $\sigma \simeq 1.4d$ (the red dashed line). The lattice depth V_L is slowly ramped up for a duration $t_{\rm ramp} = 20\hbar/E_r^{\rm eff}$ from $V_L = 0$ to $V_L = V_L^0$, and lattice parameters $N = 4$, $V_L^0 = V_B = \hbar\Omega = 200E_r^{\rm eff}$. The atom density after loading is spatially modulated, with a period $d/4$ (the blue line). (b) Evolution of the density distribution during Bloch oscillations, calculated for the dynamic lattice parameters of (a), and for a force $F = W_{\rm eff}/(8d_{\rm eff})$, where $W_{\rm eff} \simeq 0.06E_r^{\rm eff}$ is the expected bandwidth of the lowest band for $U_{\rm eff} = 10.9E_r^{\rm eff}$. (c) Evolution of the center-of-mass position during Bloch oscillations, calculated for a standard optical lattice of depth $U_{\rm eff} = 10.9E_r^{\rm eff}$ (the red dashed line), and for the dynamic optical lattice (the blue line). The time and spatial coordinates are plotted in units of the ideal Bloch period $\tau_B = 2N\hbar k/F$ and amplitude $W_{\rm eff}/F$.

reference moving at the velocity $v = v_{\text{latt}}$, where the potential $V(x' = x - vt, t)$ consists of the sum of a modulated magnetic field and a very deep static lattice $V_L \cos(2kx')\sigma_z$, with $V_L \sim \hbar\Omega \gg U_{\text{eff}}$. Both points of view can be reconciled by a proper interpretation of the band structure, as illustrated for the case $N = 2$ in Fig. 4. Among the eigenenergies $\omega(\tilde{q})$ calculated numerically in the laboratory frame $v = 0$, we identify the Bloch bands corresponding to a static effective lattice of spacing d_{eff}. The eigenenergies $\omega'(\tilde{q})$ corresponding to a frame of reference moving at a velocity v can be deduced from those in the laboratory frame using the relation $\omega' = \omega - \tilde{q}v/\hbar$. In the frame moving at $v = v_{\text{latt}}$, we observe Bloch bands corresponding to a very deep static optical lattice of period d.

We now consider a 2D extension of our scheme. The time-dependent part of the Hamiltonian is taken as

$$\begin{aligned} V(\mathbf{r}, t) = {} & V_L \cos(2k\boldsymbol{e}_1 \cdot \mathbf{r} - \Omega_1 t)\sigma_z + V_B \cos(N\Omega_1 t)\sigma_x \\ & + V_L \cos(2k\boldsymbol{e}_2 \cdot \mathbf{r} - \Omega_2 t)\sigma_x + V_B \cos(N\Omega_2 t)\sigma_y \\ & + V_L \cos(2k\boldsymbol{e}_3 \cdot \mathbf{r} - \Omega_3 t)\sigma_y + V_B \cos(N\Omega_3 t)\sigma_z, \end{aligned}$$

where the unit vectors $\boldsymbol{e}_{1,2,3}$ have directions as represented in Fig. 5. For a suitable choice of the frequencies $\Omega_{1,2,3}$ [28], each line of the equation above can be treated individually, which results in an effective potential of the form [29]

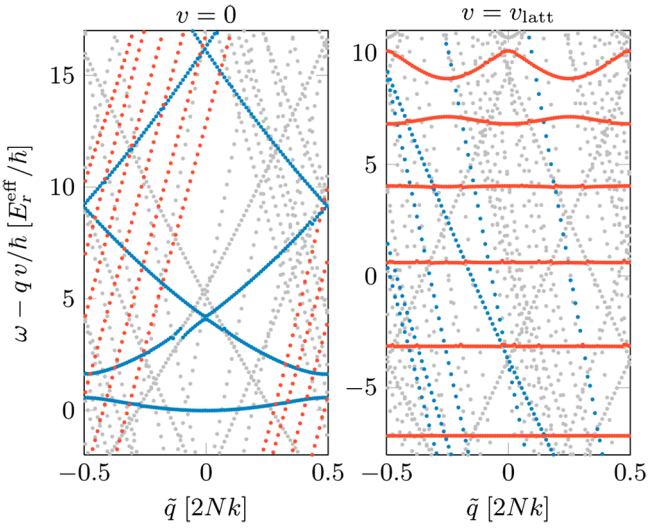

FIG. 4 (color online). Band structure corresponding to the dynamic lattice for the parameters $N = 2$, $V_L = V_B = \hbar\Omega = 10E_r^{\text{eff}}$. The panels correspond to different frames of reference, of velocity $v = 0$ (left panel) and $v = v_{\text{latt}} = \Omega/(2k)$ (right panel). The blue points correspond to the band structure of an optical lattice of spacing $d_{\text{eff}} = d/N$ and depth $U_{\text{eff}} \simeq 2E_r^{\text{eff}}$, at rest in the laboratory frame. The red dots correspond to the band structure of an optical lattice of spacing d and depth $U \simeq 74E_r$ ($\simeq 9U_{\text{eff}}$), at rest in the frame of velocity $v = v_{\text{latt}}$ [27].

$$V_{\text{eff}}(\mathbf{r}) \simeq \frac{U_{\text{eff}}}{2}[\cos(2Nk\boldsymbol{e}_1 \cdot \mathbf{r})\sigma_x + \cos(2Nk\boldsymbol{e}_2 \cdot \mathbf{r})\sigma_y + \cos(2Nk\boldsymbol{e}_3 \cdot \mathbf{r})\sigma_z], \quad (6)$$

where N is taken to be an even integer. These couplings are illustrated in quasimomentum space in Fig. 5(a). Following Ref. [30], the topological Chern number associated with the lowest energy band can be readily obtained from these couplings. Indeed, the Chern number measures the flux of the Berry curvature $\Omega(\boldsymbol{q})$ over the entire (momentum-space) unit cell:

$$\nu_{\text{Ch}} = \frac{1}{2\pi}\int_{\text{unit cell}} \Omega(\boldsymbol{q}) d^2q, \quad (7)$$

which can be directly evaluated by calculating the phases accumulated by a state as it performs a loop around the triangular subcells [30]. For the effective lattice described by Eq. (6), each unit cell is constituted of four triangular subcells, and we find an accumulated phase of $\pi/2$ within each of them [see Fig. 5(b)]. In this configuration, the Chern number of the lowest band is given by $\nu_{\text{Ch}} = (1/2\pi) \times 4 \times (\pi/2) = 1$. Generally, the reasoning above is valid only in the weak-binding regime; however, for the coupling (6), ν_{Ch} is unchanged for all values of U_{eff}. Note that the size of the unit cell in real space scales as $1/N^2$; we thus expect the flux density to be increased by a factor of N^2 compared to standard optical lattices.

The method discussed above is based on applying strong spin-dependent optical lattices, for which Lanthanide atoms would be most suited for a practical implementation.

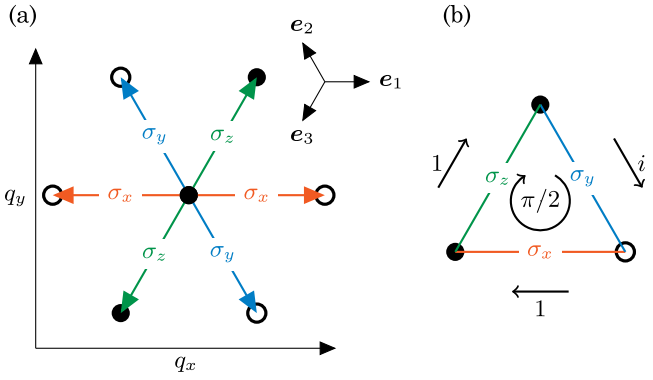

FIG. 5 (color online). (a) Momentum-space representation of the effective couplings in Eq. (6), illustrated as arrows of length $2Nk$, oriented along the unit vectors $\pm\boldsymbol{e}_i$ ($i = 1, 2, 3$), and proportional to Pauli matrices. Quantum states are represented in the basis $\{|+_z\rangle$ (the filled dots), $|-_z\rangle$ (the circles)$\}$. (b) Phase accumulated around a triangular subcell of the k-space lattice. Because of the internal-state degree of freedom, the unit cell of the lattice is formed by four triangular subcells. The same phase of $\phi = \pi/2$ is found to be accumulated around all subcells, indicating that the lowest energy band is associated with a nontrivial Chern number $\nu_{\text{Ch}} = 1$ [30].

Indeed, the optical lattices could be generated using laser light close to a narrow optical transition, which would lead to deep, spin-dependent lattices with negligible Rayleigh scattering effects (for Dy atoms, one can achieve ratios $\hbar\Gamma_{\text{scattering}}/V_L \sim 10^{-7}$) [31–33].

In conclusion, we introduced a novel scheme to engineer spatially periodic atom traps of subwavelength spacing, based on the application of spin-dependent optical lattices. A natural extension of this work would be to include interactions between atoms in the effective lattice description, and to understand whether micromotion plays a significant role in scattering properties [34–36]. This aspect will play a central role for investigating quantum many-body physics with short-spacing lattices.

The authors are pleased to acknowledge Fabrice Gerbier and Jérôme Beugnon for valuable discussions. This work is supported by IFRAF, ANR (ANR-12-BLANAGAFON), ERC (Synergy UQUAM), the Royal Society of London, and the EPSRC. N. G. is financed by the FRS-FNRS Belgium and by the BSPO under PAI Project No. P7/18 DYGEST.

*sylvain.nascimbene@lkb.ens.fr

[1] M. Lewenstein, A. Sanpera, V. Ahufinger, B. Damski, A. Sen, and U. Sen, Adv. Phys. **56**, 243 (2007).
[2] I. Bloch, J. Dalibard, and W. Zwerger, Rev. Mod. Phys. **80**, 885 (2008).
[3] J. Sebby-Strabley, M. Anderlini, P. S. Jessen, and J. V. Porto, Phys. Rev. A **73**, 033605 (2006).
[4] S. Fölling, S. Trotzky, P. Cheinet, M. Feld, R. Saers, A. Widera, T. Müller, and I. Bloch, Nature (London) **448**, 1029 (2007).
[5] P. Soltan-Panahi, J. Struck, P. Hauke, A. Bick, W. Plenkers, G. Meineke, C. Becker, P. Windpassinger, M. Lewenstein, and K. Sengstock, Nat. Phys. **7**, 434 (2011).
[6] L. Tarruell, D. Greif, T. Uehlinger, G. Jotzu, and T. Esslinger, Nature (London) **483**, 302 (2012).
[7] W. Yi, A. Daley, G. Pupillo, and P. Zoller, New J. Phys. **10**, 073015 (2008).
[8] B. Dubetsky and P. R. Berman, Phys. Rev. A **66**, 045402 (2002).
[9] G. Ritt, C. Geckeler, T. Salger, G. Cennini, and M. Weitz, Phys. Rev. A **74**, 063622 (2006).
[10] M. Gullans, T. G. Tiecke, D. E. Chang, J. Feist, J. D. Thompson, J. I. Cirac, P. Zoller, and M. D. Lukin, Phys. Rev. Lett. **109**, 235309 (2012).
[11] J. Thompson, T. Tiecke, N. de Leon, J. Feist, A. Akimov, M. Gullans, A. Zibrov, V. Vuletić, and M. Lukin, Science **340**, 1202 (2013).
[12] O. Romero-Isart, C. Navau, A. Sanchez, P. Zoller, and J. I. Cirac, Phys. Rev. Lett. **111**, 145304 (2013).
[13] P. Avan, C. Cohen-Tannoudji, J. Dupont-Roc, and C. Fabre, J. Phys. (Paris) **37**, 993 (1976).
[14] S. Rahav, I. Gilary, and S. Fishman, Phys. Rev. A **68**, 013820 (2003).
[15] N. Goldman and J. Dalibard, Phys. Rev. X **4**, 031027 (2014).
[16] M. Bukov, L. D'Alessio, and A. Polkovnikov, Adv. Phys. **64**, 139 (2015).
[17] N. Goldman, G. Juzeliūnas, P. Ohberg, and I. B. Spielman, Rep. Prog. Phys. **77**, 126401 (2014).
[18] E. J. Bergholtz and Z. Liu, Int. J. Mod. Phys. B **27**, 1330017 (2013).
[19] S. A. Parameswaran, R. Roy, and S. L. Sondhi, C.R. Phys. **14**, 816 (2013).
[20] See Supplemental Material at http://link.aps.org/supplemental/10.1103/PhysRevLett.115.140401, which includes Refs. [21–23], for a discussion on the stroboscopic method, the calculation of the effective potential, the Bloch-Floquet calculation, the resummation of the perturbative expansion of H_{eff}, micromotion effects in momentum space, and the description of the lattice loading.
[21] P. Hauke, O. Tieleman, A. Celi, C. Ölschläger, J. Simonet, J. Struck, M. Weinberg, P. Windpassinger, K. Sengstock, M. Lewenstein *et al.*, Phys. Rev. Lett. **109**, 145301 (2012).
[22] N. Goldman, J. Dalibard, M. Aidelsburger, and N. R. Cooper, Phys. Rev. A **91**, 033632 (2015).
[23] J. H. Denschlag, J. Simsarian, H. Häffner, C. McKenzie, A. Browaeys, D. Cho, K. Helmerson, S. Rolston, and W. Phillips, J. Phys. B **35**, 3095 (2002).
[24] M. Holthaus, Z. Phys. B **89**, 251 (1992).
[25] M. Grifoni and P. Hänggi, Phys. Rep. **304**, 229 (1998).
[26] This depth value slightly differs from the perturbative result $U_{\text{eff}} \simeq 16.7E_r^{\text{eff}}$, from Eq. (4), since $V_{L,B} \sim \hbar\Omega$. We checked numerically that the difference can be accounted for by higher-order terms.
[27] The modulated magnetic field $V_B \cos(N\Omega t)\sigma_x$ renormalizes the depth U of the optical lattice according to $U = 2J_0[V_B/(N\hbar\Omega)]V_L$, as observed in the calculated band structures.
[28] The frequencies $\Omega_{1,2,3}$ should not be chosen to be too close to each other, and their ratios should not approach simple fractions.
[29] N. R. Cooper, Phys. Rev. Lett. **106**, 175301 (2011).
[30] N. R. Cooper and R. Moessner, Phys. Rev. Lett. **109**, 215302 (2012).
[31] S. Nascimbene, J. Phys. B **46**, 134005 (2013).
[32] X. Cui, B. Lian, T.-L. Ho, B. L. Lev, and H. Zhai, Phys. Rev. A **88**, 011601 (2013).
[33] J. Dalibard, in *Quantum Matter at Ultralow Temperatures, Proceedings of the International School of Physics "Enrico Fermi," Course CXCI* (IOS Press, Amsterdam, 2014).
[34] S. Choudhury and E. J. Mueller, Phys. Rev. A **90**, 013621 (2014).
[35] T. Bilitewski and N. R. Cooper, Phys. Rev. A **91**, 033601 (2015).
[36] A. Eckardt and E. Anisimovas, arXiv:1502.06477.